

Destruction of surface states of $(d_{zx} + id_{yz})$ -wave superconductor by surface roughness: application to Sr_2RuO_4

Shu-Ichiro Suzuki,^{1,*} Satoshi Ikegaya,² and Alexander A. Golubov¹

¹MESA+ Institute for Nanotechnology, University of Twente, 7500 AE Enschede, The Netherlands

²Department of Applied Physics, Nagoya University, Nagoya 464-8603, Japan

(Dated: July 12, 2022)

The fragility of the chiral surface current of $(d_{zx} + id_{yz})$ -wave superconductor, a potential candidate for Sr_2RuO_4 , against surface roughness is demonstrated utilizing the quasiclassical Eilenberger theory. Comparing the chiral surface currents of $(d_{zx} + id_{yz})$ -wave and $(p_x + ip_y)$ -wave pairings, we conclude the chiral current for $(d_{zx} + id_{yz})$ -wave SC is much more fragile than that for the $(p_x + ip_y)$ -wave one. The difference can be understood in terms of the orbital symmetry of the odd-frequency Cooper pairs arising at the surface. Our results show the $(d_{zx} + id_{yz})$ -wave scenario can explain the null spontaneous magnetization in Sr_2RuO_4 experiments.

Introduction.—The determination of the pairing symmetry in Sr_2RuO_4 (SRO) superconductors (SCs) has been an unsolved problem for more than a quarter century^{1–4}. In the last few years, nevertheless, researchers in this field undergo a remarkable paradigms shift. Specifically, recent precise experiments on spin susceptibility^{5–8} appear to contradict a spin-triplet odd-parity superconducting state with broken time-reversal symmetry (TRS)⁹, which had heretofore been the leading candidate in SRO. Alternatively, an exotic *inter-orbital-singlet* spin-triplet even-parity state with broken time-reversal symmetry has come under the spotlight^{10,11} because it can explain recent two remarkable experimental observations, i.e., a sharp jump in the shear elastic constant c_{66} at the superconducting transition temperature measured by ultrasound experiments^{12,13}, and a stress-induced split between the onset temperatures for the superconducting state and broken TRS state measured by muon spin-relaxation experiments^{14,15}. Nowadays, careful and intensive verification for the realization of the inter-orbital superconducting state in SRO has been underway.

On the basis of a microscopic model for the inter-orbital superconducting state of SRO¹⁰, the superconducting gap on the three Fermi surfaces of SRO has a $(d_{zx} + id_{yz})$ -wave pairing symmetry (i.e., $d + id'$ -wave SC). It has been shown that the $d + id'$ -wave SC hosts characteristic surface states^{16–19}. At material surfaces parallel to the z -axis (i.e. the c -axis of the SRO), the $d + id'$ -wave SC exhibits dispersing chiral surface states due to the chiral pairing symmetry with fixed k_z . Moreover, the pure odd-parity nature with respect to k_z results in the emergence of dispersion-less zero-energy surface states at the surfaces perpendicular to the z -axis. Thus, observations of these surface states can be the conclusive evidence for the inter-band superconducting state in SRO. However, scanning superconducting quantum interference device experiments^{20,21} have not detected the expected spontaneous edge current due to the chiral surface states^{22–27}, and tunneling spectroscopy measurements along the z -axis did not observe a zero-bias conductance peak suggesting the dispersion-less zero-energy

surface states^{28–30}. Therefore, when we take the experimental observations at face value, the inter-orbital superconducting state with a $d + id'$ -wave superconducting gap seems to be excluded.

In this Letter, we study the influence of surface roughness on the surface states of the $d + id'$ -wave SC. The most straightforward numerical simulation is adding random potentials to the microscopic three-orbital Hamiltonian¹⁰. However, such numerical simulation requires significantly large systems in real-space, ensemble averaged of impurity configurations, and self-consistent treatments for the order parameter, meaning that it would be impossible to implement owing to the prohibitive numerical costs. Alternatively, we employ the quasiclassical Eilenberger theory for a simple single-band and clarify essential properties of the surface states of the $d + id'$ -wave SC. As a result, we demonstrate that the surface current due to the chiral surface states and the sharp zero-energy peak in the surface density of states due to the dispersion-less zero-energy surface states are easily destroyed by surface roughness. Importantly, the vulnerability of the surface states is owing to a roughness-induced destructive interference effect which is inevitable with the $d + id'$ -wave pairing symmetry. Namely, the surface states of the $d + id'$ -wave SC in the presence of surface roughness are fragile regardless of details of the model.

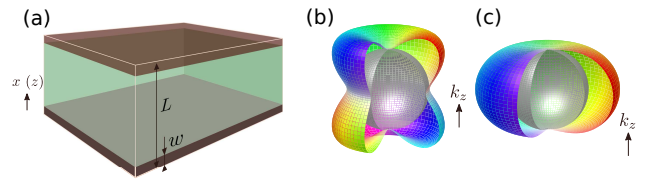


FIG. 1. (a) Schematics of the system. The surfaces are parallel to the either of x or z axis. The widths of the superconductor and disordered regions are denoted by L and w . The translational symmetry is assumed in the direction parallel to the surfaces. The pair potentials of $(d_{zx} + id_{yz})$ - and $(p_x + ip_y)$ -wave superconductors are shown in (b) and (c). The colour indicates $\arg[\Delta(k)]$. The inner silver sphere represents the Fermi sphere.

We will conclude that the absence of experimental signatures from the surface states does not contradict with the inter-orbital $d + id'$ -wave superconducting states in SRO because surface roughness is inevitable in real-life experiments.

Quasiclassical Eilenberger theory.— We examine the effects of surface roughness utilizing the quasiclassical Eilenberger theory³¹. The SC has a pair of parallel surfaces which are perpendicular to the x or z axis as shown in Fig. 1(a). The thin dirty layers with the width w are introduced. The Green's functions obey the Eilenberger equation:

$$i\mathbf{v}_F \cdot \nabla \check{g} + [i\omega_n \check{\tau}_3 + \check{H}, \check{g}]_- = 0, \quad (1)$$

$$\check{H} = \check{\Delta} + \check{\Sigma} = \begin{pmatrix} \hat{\xi} & \hat{\eta} \\ \hat{\eta} & \hat{\xi} \end{pmatrix}, \quad \check{\Sigma} = \frac{i}{2\tau_0} \langle \check{g} \rangle, \quad (2)$$

$$\check{g} = \begin{pmatrix} \hat{g} & \hat{f} \\ -\hat{f} & -\hat{g} \end{pmatrix}, \quad \check{\Delta} = \begin{pmatrix} 0 & \hat{\Delta} \\ \hat{\Delta} & 0 \end{pmatrix}, \quad (3)$$

where $\langle \cdots \rangle = \int_0^\pi \int_{-\pi}^\pi \cdots \sin \theta d\varphi d\theta / 4\pi$, $\check{g} = \check{g}(\mathbf{r}, \mathbf{k}, i\omega_n)$ is the quasiclassical Green's function in the Mastubara representation, $\hat{\Delta} = \hat{\Delta}(\mathbf{r}, \mathbf{k})$ is the pair-potential matrix, $\check{\Sigma} = \check{\Sigma}(\mathbf{r}, i\omega_n)$ is the self-energies by the impurity scatterings, and we assume the system is in equilibrium. The mean free path is denoted $\ell = v_F \tau_0$ with τ_0 being the mean free time that is fixed at a certain value in the disordered region but infinitely large in the other place. In this Letter, the accents $\check{\cdot}$ and $\hat{\cdot}$ means matrices in particle-hole and spin space. The identity matrices in particle-hole and spin space are respectively denoted by $\check{\tau}_0$ and $\hat{\sigma}_0$. The Pauli matrices are denoted by $\check{\tau}_j$ and $\hat{\sigma}_j$ with $j \in 1, 2, 3$. All of the functions satisfies the symmetry relation $\hat{K}(\mathbf{r}, \mathbf{k}, i\omega_n) = [\hat{K}(\mathbf{r}, -\mathbf{k}, i\omega_n)]^*$, where the unit vector \mathbf{k} represents the direction of the Fermi momentum. Effects of the vector potential are ignored because it affects on surface states only quantitatively.

The Eilenberger equation (1) can be simplified by the so-called Riccati parameterization^{32–34}. The Green's function can be expressed in terms of the coherence function $\hat{\gamma} = \hat{\gamma}(\mathbf{r}, \mathbf{k}, i\omega_n)$:

$$\check{g} = 2 \begin{pmatrix} \hat{G} & \hat{F} \\ -\hat{F} & -\hat{G} \end{pmatrix} - \check{\tau}_3, \quad (4)$$

$$\hat{G} = (1 - \hat{\gamma}\hat{\gamma})^{-1}, \quad \hat{F} = (1 - \hat{\gamma}\hat{\gamma})^{-1}\hat{\gamma}. \quad (5)$$

The equation for $\hat{\gamma}$ is given by

$$(i\mathbf{v}_F \cdot \nabla + 2i\omega_n)\hat{\gamma} + \hat{\xi}\hat{\gamma} - \hat{\gamma}\hat{\xi} - \hat{\eta} + \hat{\gamma}\hat{\eta}\hat{\gamma} = 0. \quad (6)$$

Assuming no spin-dependent potential and single-spin $\hat{\Delta}$,

we can parameterize the spin structure of the functions:

$$\hat{\Delta} = i\Delta_{\mathbf{k},\nu}(i\hat{\sigma}_\nu\hat{\sigma}_2), \quad (7)$$

$$\hat{\Delta} = -i\Delta_{-\mathbf{k},\nu}^*(i\hat{\sigma}_\nu\hat{\sigma}_2)^* = i\Delta_{\mathbf{k},\nu}^*(i\hat{\sigma}_\nu\hat{\sigma}_2)^\dagger \quad (8)$$

$$\hat{g} = g\hat{\sigma}_0, \quad \hat{f} = f_\nu(i\hat{\sigma}_\nu\hat{\sigma}_2), \quad \hat{f} = \tilde{f}_\nu(i\hat{\sigma}_\nu\hat{\sigma}_2)^\dagger, \quad (9)$$

$$\hat{\eta} = i\eta_\nu(i\hat{\sigma}_\nu\hat{\sigma}_2), \quad \hat{\eta} = i\tilde{\eta}_\nu(i\hat{\sigma}_\nu\hat{\sigma}_2)^\dagger, \quad (10)$$

where $\nu = 0$ ($\nu \in \{1, 2, 3\}$) is for the spin-singlet (spin-triplet) SC. In the following, we make ν explicit only when necessary. Equation (6) can be reduced to

$$\mathbf{v}_F \cdot \nabla \gamma + 2\tilde{\omega}\gamma - \eta + \tilde{\eta}\gamma^2 = 0, \quad (11)$$

$$\tilde{\omega} = \omega_n + \frac{\text{Re}\langle g \rangle}{2\tau_0}, \quad (12)$$

$$\eta_\nu = \Delta_{\mathbf{k}} + \frac{\langle f \rangle}{2\tau_0}, \quad \tilde{\eta}_\nu = \Delta_{\mathbf{k}}^* - S_\nu \frac{\langle f \rangle^*}{2\tau_0}. \quad (13)$$

The coherence functions in the homogeneous limit $\bar{\gamma}$ is given by

$$\bar{\gamma}(\mathbf{k}, i\omega_n) = \frac{s_o \Delta_{\mathbf{k}}}{|\omega_n| + \sqrt{\omega_n^2 + |\Delta_{\mathbf{k}}|^2}}, \quad (14)$$

with $s_o = \text{sgn}[\omega_n]$ and $\bar{\cdot}$ means the bulk value.

The momentum dependence of the pair potential is assumed as

$$\Delta_{\mathbf{k}} = \begin{cases} 2(\Delta_1 k_x + i\Delta_2 k_y)k_z & \text{for } d + id'\text{-wave,} \\ \Delta_1 k_x + i\Delta_2 k_y & \text{for } p + ip'\text{-wave,} \end{cases} \quad (15)$$

where we put the factor 2 in the $d + id'$ -wave case such that $\max[\Delta_{\mathbf{k}}] = \bar{\Delta}$ in the homogeneous limit. The schematic gap amplitudes in the bulk are shown in Fig. 1(b) and 1(c), where the color means the phase of the pair potential $\arg[\Delta(\mathbf{k})]$. The spatial dependence of the pair potentials are determined by the self-consistent gap equation which relates f and Δ :

$$\Delta_\mu(\mathbf{r}) = 2\lambda N_0 \frac{\pi}{i\beta} \sum_{\omega_n} \langle V_\mu(\mathbf{k}') f(\mathbf{r}, \mathbf{k}', i\omega_n) \rangle, \quad (16)$$

$$\lambda = \frac{1}{2N_0} \left[\ln \frac{T}{T_c} + \sum_{n=0}^{n_c} \frac{1}{n + 1/2} \right]^{-1}, \quad (17)$$

where $\mu = 1$ or 2 , $\beta = 1/T$, T_c is the critical temperature, N_0 is the density of the states (DOS) in the normal state at the Fermi energy, and n_c is the cut-off integer. The corresponding attractive potentials are $(V_1, V_2) = (15/2)(k_z k_x, k_y k_z)$ for the $d + id'$ -wave and $(V_1, V_2) = 3(k_x, k_y)$ for the $p + ip'$ -wave SCs.

The charge current, local DOS, and angle-resolved

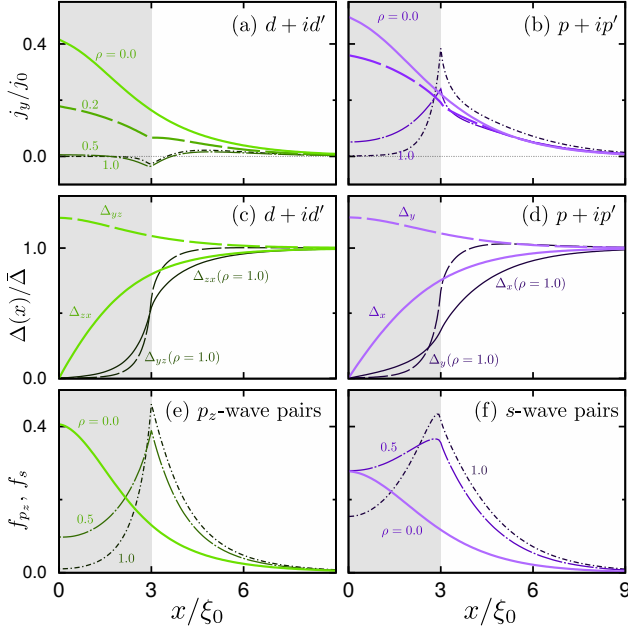


FIG. 2. Calculated results for the (a)(c)(e) $d + id'$ -wave and (b)(d)(f) $p + ip'$ -wave SCs. (a)-(b) The edge-current density in the y direction, (c)-(d) self-consistent pair potentials Δ , and (e)-(f) subdominant pair amplitudes are shown. The surface-roughness parameters are fixed as $\rho = \xi_0/\ell$ and $w = 3\xi_0$. The current density is normalized to $j_0 = |e|v_F N_0 \pi T_c$.

DOS are calculated from the Green's function:

$$j_y(\mathbf{r}) = eN_0 \frac{\pi}{i\beta} \sum_{\omega_n} \langle k_y \text{Tr} [\tilde{\tau}_3 \tilde{g}(\mathbf{r}, \mathbf{k}, i\omega_n)] \rangle, \quad (18)$$

$$N(\mathbf{r}, E) = \int N_{\text{AR}}(\mathbf{r}, k_y, E) dk_{\parallel}, \quad (19)$$

$$\frac{N_{\text{AR}}}{N_0} = \sum_{\alpha=\pm 1} \text{Re}[g(\mathbf{r}, \pm k_{\perp}, \mathbf{k}_{\parallel}, i\omega_n)]_{i\omega_n \rightarrow E+i\delta}, \quad (20)$$

with $e < 0$ is the charge of an electron, \mathbf{k}_{\parallel} (k_{\perp}) is the momentum parallel (perpendicular) to the surface. The amplitude of the subdominant Cooper pairs can be extracted from the anomalous Green's function:

$$f_{p_z} = \langle k_z f \rangle, \quad f_s = \langle f \rangle, \quad (21)$$

In the numerical simulations, we fix the parameters: $L = 80\xi_0$, $w = 3\xi_0$, $\omega_c = 10\pi T_c$, $T = 0.2T_c$, $\delta = 0.01\bar{\Delta}$ with $\xi_0 = \hbar v_F / 2\pi T_c$ being the coherence length.

Chiral surface current and pair functions.—We first discuss the result for the open surface in the x -axis direction. The spatial profiles of j_y and Δ are shown in 2(a)-2(d), where the results for the $d + id'$ -wave and $p + ip'$ -wave SCs are shown in the left and right panels respectively. Figures 2(a) and 2(b) show the chiral surface current (CSC) for the $d + id'$ -wave SC is much more sensitive to the surface roughness than the $p + ip'$ -wave case. Even with a weak surface roughness (i.e.,

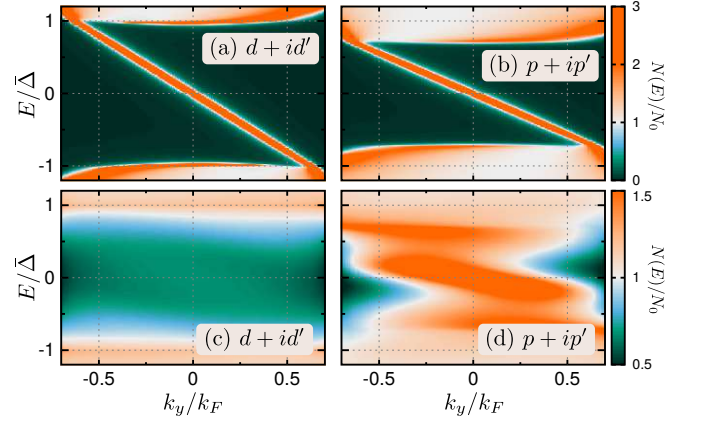


FIG. 3. Angle-resolved density of states at $k_z/k_F = 1/\sqrt{2}$ for the (a)(c) $d + id'$ -wave and (b)(d) $p + ip'$ -wave SCs. The results are obtained at $x = 0$ for the clean case [(a) and (b)] and at $x = w$ for the rough case with $\xi_0/\ell = 0.5$ [(c) and (d)]. The ARDOS are normalized to its value in the normal state.

$\xi_0/\ell = 0.5$), the CSC for the $d + id'$ -wave SC is almost zero[?], whereas that for the $p + ip'$ -wave SC is sufficiently large to be observed^{26,27} where the peak in the current density moves from the surface to the internal surface between the disordered and ballistic regions. The pair potentials for the both SCs show qualitatively the same behaviour to the surface roughness. At the clean surface, the component that changes its sign during the reflection (i.e., Δ_{zx} and Δ_x) becomes zero as shown in Figs. 2(c) and 2(d). Correspondingly, the other component is enhanced. When the surface is rough, both of the components are strongly suppressed due to the random scatterings.

The difference in the robustness of the CSC comes from the symmetry of the subdominant Cooper pairs induced by the local inversion symmetry breaking at a surface. The inversion-symmetry breaking results in the parity mixing of the pair amplitudes³⁵. Namely, odd-parity (even-parity) pairings are induced at a surface of the $d + id'$ -wave ($p + ip'$ -wave) SC. The p_z - and s -wave pair amplitudes (i.e., subdominant pairs with the lowest azimuthal quantum number) in each SC are shown in Figs. 2(e) and 2(f), where we fix $\omega_n = \omega_0$. The s -wave subdominant pairs plays an important role under an disordered potential, whereas p_z -wave does not. The s -wave pairs $\langle f \rangle$ act as an effective pair potential in a disordered region [See Eq. (13)]. Namely, the disordered region of the $p + ip'$ -wave SC becomes an effective s -wave SC rather than a normal metal. Consequently, the chiral current of the $p + ip'$ -wave SC flows along the internal interface at $x = w$. In Appendix, we show that \tilde{g} at the internal interface is qualitatively the same as that at a surface of a p -wave SC. The chiral current does not flow at the internal interface in $d + id'$ -wave cases because the anisotropic p_z -wave pairs can not act as an effective pair potential [i.e., $\langle f \rangle = 0$ in Eq. (13)].

The angle-resolved DOS (ARDOS) for the $d + id'$ - and

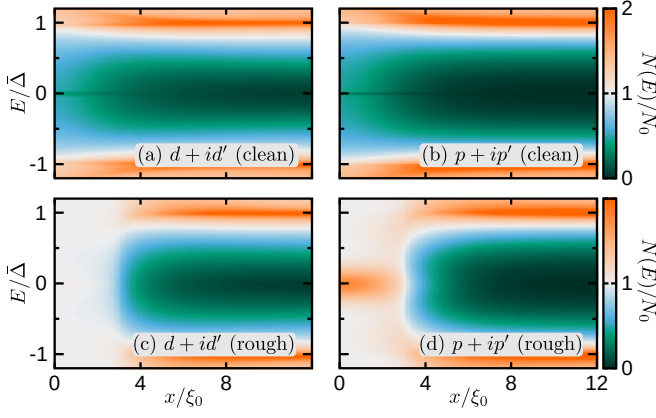


FIG. 4. Local density of states of the (a)(c) $d + id'$ -wave and (b)(d) $p + ip'$ -wave SCs. The surface roughness is set to $\xi_0/\ell = 0.5$ and $w = 3\xi_0$ in (c) and (d). The LDOS at $x = 0$ is enhanced because of the chiral surface states. In $d + id'$ -wave case, the disordered region can be regarded as a normal metal [i.e., $N(E) = N_0$]. The LDOS is normalized to its value in the normal state N_0 .

$p + ip'$ -wave SCs are compared in Fig. 3, where we fix $k_z = k_F/\sqrt{2}$. The ARDOS with $\rho = 0$ ($\rho = 0.5$) are obtained at the surface (internal interface). In the clean limit, the chiral surface states are prominent in each SC. When the surface is rough, the chiral states for the $d + id'$ -wave SC vanishes [Fig. 3(c)], whereas that for the $p + ip'$ -wave SC is robust [Fig. 3(d)]. The LDOS can be calculated by integrating ARDOS. The results are shown in Fig. 4. We see the chiral surface states appear at the surface; the LDOS increases at the surface (light blue region) as shown in Figs. 4(a) and 4(b). Under the surface roughness, $N(x, E) = N_0$ in the disordered region of the $d + id'$ -wave case, meaning that the disordered region becomes a normal metal. In the $p + ip'$ -wave SC, on the contrary, the LDOS has a peak structure in the disordered region, reflecting the emergence of the effective s -wave superconductivity in the disordered region. To detect the chiral surface states of the $d + id'$ -wave SC, one has to pay close attention to the surface quality because they are very sensitive to the roughness.

Andreev bound states at c -axis surface.—At the surface in the c -axis direction of the $d + id'$ -wave SC, the dispersion-less zero-energy states (ZESs) appear.^{16–18} The effects of the surface roughness are shown in Fig. 5, where we also show the results for a p_z -wave SC (i.e., polar state with $\Delta_{\mathbf{k}} \sim p_z$) as a reference³⁶. The ZESs for both SCs are prominent in the clean limit [Figs. 5(a) and 5(d)]. However, in the $d + id'$ -wave case, the ZESs become broader even by weak surface roughness (e.g., $\xi_0/\ell = 0.2$). Contrary to the p_z -wave SC^{37–39}, the ZESs of the $d + id'$ -wave SC disappear even for the weak disorder (i.e., $\xi_0 < \ell$).

The fragility of the ZESs can be explained by the absence of the s -wave subdominant pairs $\langle f \rangle$. The p_z -wave SC has robust ZESs supported by the s -wave pairs³⁸ (i.e.,

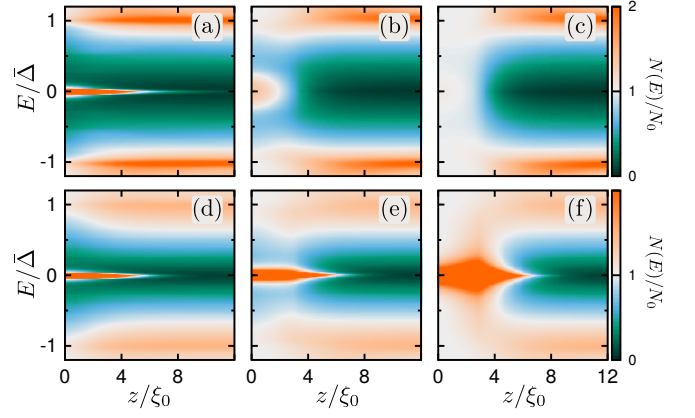


FIG. 5. Effects of the surface roughness on the dispersion-less surface states of (a)–(c) the $d + id'$ -wave and (d)–(f) p_z -wave SCs. The surface is perpendicular to the z axis. The strength of the roughness is set to (a)(d) $\xi_0/\ell = 0.0$, (b)(e) 0.2, and (c)(f) 0.5. The results are obtained from the self-consistent Δ (not shown). The surface state in the z direction of $d + id'$ -wave case is much more fragile than those of p_z -wave case.

effective pair potential). On the other hand, the subdominant pairs for the $d + id'$ -wave SC are $p_x + ip_y$ -wave-like pairs because of the phase winding at a fixed k_z . Anisotropic $p_x + ip_y$ -wave pairs do not act as an effective pair potential [i.e., $\langle f \rangle = 0$ in Eq. (13)]. Therefore, the ZES at a surface in the c -axis direction of a $d + id'$ -wave SC are fragile against roughness.

Discussion.—The important factor determining the robustness of surface states is only the presence of subdominant s -wave pairing induced at a surface. Therefore, we can generalize our knowledge to higher order chiral superconductors. We have confirmed that the chiral surface states of $f_{x(5z^2-1)} + if'_{y(5z^2-1)}$ -wave SC are fragile against roughness because of the absence of the s -wave pairs. Similarly, we can anticipate fragile dispersion-less ZESs in the $f_{(x^2-y^2)z} + if_{xyz}$ -wave SC since no s -wave pairing is expected.

In this Letter, we employ the simple single-band model and ignore the multi-orbital nature of SRO. The fragility of the surface states is owing to the absence of s -wave Cooper pairs at the surface. In a $d + id$ -wave SC, such s -wave subdominant pairs can be induced only in extreme cases: the scatterings by roughness cause a constructive interference for s -wave pairs. Therefore, the fragility of the surface states of the $d + id'$ -wave SC would be irrelevant to the details of the model. Studying the roughness effects in detail with more realistic three-orbital models¹⁰ would be an important future task, where the surface states would be suffered additionally from more complicated inter-band scatterings.

Here we briefly note that there are several experimental findings that appears to contradict the $d + id'$ -wave states in SRO. For instance, a recent specific-heat measurement suggests the absence of split between the onset temperatures for the superconductivity and broken time-reversal

symmetry state⁴⁰, which seems to contradict the two-component superconducting state. Moreover, a recent Josephson current measurement implies a time-reversal invariant superconducting state⁴¹. Resolving such inconsistencies remains as an important future task.

Conclusion.— We have investigated the effects of surface roughness on the surface states of the $(d_{zx} + id_{yz})$ -wave SC. Utilizing the quasiclassical Eilenberger theory, we have demonstrated that the surface states of the $(d_{zx} + id_{yz})$ -wave SC are easily destroyed by surface roughness. Since the surface roughness is inevitable in real-life experiments, the absence of the experimental signatures from the surface states^{20,21,28–30} would not be clearly inconsistent with the inter-orbital $(d_{zx} + id_{yz})$ -wave superconducting state in SRO¹⁰.

ACKNOWLEDGMENTS

We are grateful to A. Brinkman, Y. Asano, and T. Kikkeler for the fruitful discussions. S.-I. S. is supported by JSPS Postdoctoral Fellowship for Overseas Researchers and a Grant-in-Aid for JSPS Fellows (JSPS KAKENHI Grant No. JP19J02005), and thanks the University of Twente for hospitality. S. I. is supported by a Grant-in-Aid for JSPS Fellows (JSPS KAKENHI Grant No. JP21J00041).

Appendix A: Effects of self-energy in a DN attached to a p -wave SC

In this section, we consider a simplified theoretical model: the interface between a dirty normal metal (DN) and a p -wave SC. For simplicity, we ignore the spatial

dependence of the Green's functions near the interface. The Riccati equations in the DN and SC are

$$\mathbf{v}_F \cdot \nabla \gamma_n + 2\tilde{\omega} \gamma_n - \eta + \eta \gamma_n^2 = 0, \quad (\text{A1})$$

$$\mathbf{v}_F \cdot \nabla \gamma_s + 2\omega \gamma_s - \Delta_k + \Delta_k^* \gamma_s^2 = 0. \quad (\text{A2})$$

with

$$\tilde{\omega} = \omega_n + \frac{\text{Re}\langle g \rangle}{2\tau_0}, \quad \eta = \frac{\langle f \rangle}{2\tau_0}, \quad \eta = -\frac{\langle f \rangle^*}{2\tau_0}. \quad (\text{A3})$$

At the interface, γ can be obtained:

$$\gamma_n = -\frac{1}{\eta} \left[\tilde{\omega} - \sqrt{\tilde{\omega}^2 + \eta \eta} \right], \quad \gamma_s = \frac{\Delta_k}{\omega_n + \Omega_n},$$

$$\gamma_n = \frac{1}{\eta} \left[\tilde{\omega} - \sqrt{\tilde{\omega}^2 + \eta \eta} \right], \quad \gamma_s = -\frac{\Delta_k^*}{\omega_n + \Omega_n}, \quad (\text{A4})$$

where $\Omega_n = \sqrt{\omega_n^2 + |\Delta_k|^2}$. The normal Green's function, for example, can be obtained from them:

$$g(+k, x=0, i\omega_n) = \frac{1 + \gamma_n \gamma_s(k)}{1 - \gamma_n \gamma_s(k)}, \quad (\text{A5})$$

$$g(-k, x=0, i\omega_n) = \frac{1 + \gamma_s(-k) \gamma_n}{1 - \gamma_s(-k) \gamma_n}, \quad (\text{A6})$$

The Green's functions at the surface of a semi-infinite p -wave SC are calculated from the coherence functions:

$$g_{\text{PW}}(\pm k, x=0, i\omega_n) = \frac{1 + \gamma_s(-k) \gamma_s(k)}{1 - \gamma_s(-k) \gamma_s(k)}. \quad (\text{A7})$$

Comparing Eqs. (A6) and (A7), we see the similarity when . Note that this similarity never appears in the d -, f - and g -wave SCs because $\langle f \rangle = 0$ in those SCs.

* s.suzuki-1@utwente.nl

¹ Y. Maeno, H. Hashimoto, K. Yoshida, S. Nishizaki, T. Fujita, J. G. Bednorz, and F. Lichtenberg, Superconductivity in a layered perovskite without copper, *Nature (London)* **372**, 532 (1994).

² A. P. Mackenzie and Y. Maeno, The superconductivity of Sr_2RuO_4 and the physics of spin-triplet pairing, *Rev. Mod. Phys.* **75**, 657 (2003).

³ C. Kallin and A. J. Berlinsky, Is Sr_2RuO_4 a chiral p -wave superconductor?, *J. Phys.: Condens. Matter*, **21**, 164210 (2009).

⁴ A. P. Mackenzie, T. Scaffidi, C. W. Hicks, and Y. Maeno, Even odder after twenty-three years: the superconducting order parameter puzzle of Sr_2RuO_4 , *npj Quantum Mater.* **2**, 40 (2017).

⁵ A. Pustogow, Y. Luo, A. Chronister, Y.-S. Su, D. A. Sokolov, F. Jerzembeck, A. P. Mackenzie, C. W. Hicks, N. Kikugawa, S. Raghu, E. D. Bauer, and S. E. Brown, Constraints on the superconducting order parameter in Sr_2RuO_4 from oxygen-17 nuclear magnetic resonance, *Nature* **574**, 72–75 (2019).

⁶ K. Ishida, M. Manago, and Y. Maeno, Reduction of the ^{17}O Knight Shift in the Superconducting State and the Heat-up Effect by NMR Pulses on Sr_2RuO_4 , *J. Phys. Soc. Jpn.* **89**, 034712 (2020).

⁷ A. Chronister, A. Pustogow, N. Kikugawa, D. A. Sokolov, F. Jerzembeck, C. W. Hicks, A. P. Mackenzie, E. D. Bauer, and S. E. Brown, Evidence for even parity unconventional superconductivity in Sr_2RuO_4 , *arXiv preprint arXiv:2007.13730* (2020).

⁸ A. N. Petsch, M. Zhu, M. Enderle, Z. Q. Mao, Y. Maeno, I. I. Mazin, and S. M. Hayden, Reduction of the Spin Susceptibility in the Superconducting State of Sr_2RuO_4 Observed by Polarized Neutron Scattering, *Phys. Rev. Lett.* **125**, 217004 (2020).

⁹ T. M. Rice and M. Sigrist, Sr_2RuO_4 : an electronic analogue of ^3He ?, *J. Phys.: Condens. Matter* **7** L643 (1995).

¹⁰ H. G. Suh, H. Menke, P. M. R. Brydon, C. Timm, A. Ramires, and D. F. Agterberg, Stabilizing even-parity chiral superconductivity in Sr_2RuO_4 , *Phys. Rev. Research* **2**, 032023(R) (2020).

- ¹¹ Y. Fukaya, T. Hashimoto, M. Sato, Y. Tanaka and Y. Tanaka, Spin susceptibility for orbital-singlet Cooper pair in the three-dimensional Sr_2RuO_4 superconductor, *Phys. Rev. Research* **4**, 013135 (2022).
- ¹² S. Benhabib, C. Lupien, I. Paul, L. Berges, M. Dion, M. Nardone, A. Zitouni, Z. Q. Mao, Y. Maeno, A. Georges, L. Taillefer, and C. Proust, Ultrasound evidence for a two-component superconducting order parameter in Sr_2RuO_4 , *Nat. Phys.* **17**, 194 (2021).
- ¹³ S. Ghosh, A. Shekhter, F. Jerzembeck, N. Kikugawa, D. A. Sokolov, M. Brando, A. P. Mackenzie, C. W. Hicks, and B. J. Ramshaw, Thermodynamic evidence for a two-component superconducting order parameter in Sr_2RuO_4 , *Nat. Phys.* **17**, 199 (2021).
- ¹⁴ V. Grinenko, S. Ghosh, R. Sarkar, J.-C. Orain, A. Nikitin, M. Elender, D. Das, Z. Guguchia, F. Brückner, M. E. Barber, J. Park, N. Kikugawa, D. A. Sokolov, J. S. Bobowski, T. Miyoshi, Y. Maeno, A. P. Mackenzie, H. Luetkens, C. W. Hicks, and H.-H. Klauss, Split superconducting and time-reversal symmetry-breaking transitions in Sr_2RuO_4 under stress, *Nat. Phys.* **17**, 748 (2021).
- ¹⁵ V. Grinenko, D. Das, R. Gupta, B. Zinkl, N. Kikugawa, Y. Maeno, C. W. Hicks, H.-H. Klauss, M. Sigrist, and R. Khasanov, Unsplit superconducting and time reversal symmetry breaking transitions in Sr_2RuO_4 under hydrostatic pressure and disorder, *arXiv:2103.03600*.
- ¹⁶ S. Kobayashi, Y. Tanaka, and M. Sato, Fragile surface zero-energy flat bands in three-dimensional chiral superconductors, *Phys. Rev. B* **92**, 214514 (2015).
- ¹⁷ S. Tamura, S. Kobayashi, L. Bo, and Y. Tanaka, Theory of surface Andreev bound states and tunneling spectroscopy in three-dimensional chiral superconductors, *Phys. Rev. B* **95**, 104511 (2017).
- ¹⁸ S.-I. Suzuki, M. Sato, and Y. Tanaka, Identifying possible pairing states in Sr_2RuO_4 by tunneling spectroscopy, *Phys. Rev. B* **101**, 054505 (2020).
- ¹⁹ S. Ikegaya, S.-I. Suzuki, Y. Tanaka, and D. Manske, Proposal for identifying possible even-parity superconducting states in Sr_2RuO_4 using planar tunneling spectroscopy, *Phys. Rev. Research* **3**, L032062 (2021).
- ²⁰ P. G. Björnsson, Y. Maeno, M. E. Huber, and K. A. Moler, Scanning magnetic imaging of Sr_2RuO_4 , *Phys. Rev. B* **72**, 012504 (2005).
- ²¹ J. R. Kirtley, C. Kallin, C. W. Hicks, E. -A. Kim, Y. Liu, K. A. Moler, Y. Maeno, and K. D. Nelson, Upper limit on spontaneous supercurrents in Sr_2RuO_4 , *Phys. Rev. B* **76**, 014526 (2007).
- ²² M. Matsumoto and M. Sigrist, Quasiparticle states near the surface and the domain wall in a $p_x \pm ip_y$ -wave superconductor, *J. Phys. Soc. Jpn.* **68** 3 (1999).
- ²³ A. Furusaki, M. Matsumoto and M. Sigrist, Spontaneous Hall effect in a chiral p -wave superconductor, *Phys. Rev. B* **64**, 054514 (2001).
- ²⁴ M. Stone and R. Roy, Edge modes, edge currents, and gauge invariance in $p_x + ip_y$ superfluids and superconductors, *Phys. Rev. B* **69**, 184511 (2004).
- ²⁵ Y. Nagato, S. Higashitani, and K. Nagai, Subgap in the Edge States of Two-Dimensional Chiral Superconductor with Rough Surface *J. Phys. Soc. Jpn.* **80**, 113706 (2011).
- ²⁶ S. V. Bakurskiy, A. A. Golubov, M. Yu. Kupriyanov, K. Yada, and Y. Tanaka, Anomalous surface states at interfaces in p -wave superconductors, *Phys. Rev. B* **90**, 064513 (2014).
- ²⁷ S.-I. Suzuki and Y. Asano, Spontaneous edge current in a small chiral superconductor with a rough surface, *Phys. Rev. B* **94**, 155302 (2016).
- ²⁸ H. Suderow, V. Crespo, I. Guillamon, S. Vieira, F. Servant, P. Lejay, J. P. Brison, and J. Flouquet, A nodeless superconducting gap in Sr_2RuO_4 from tunneling spectroscopy, *New J. Phys.* **11**, 093004 (2009).
- ²⁹ I. A. Firmo, S. Lederer, C. Lupien, A. P. Mackenzie, J. C. Davis, and S. A. Kivelson, Evidence from tunneling spectroscopy for a quasi-one-dimensional origin of superconductivity in Sr_2RuO_4 , *Phys. Rev. B* **88**, 134521 (2013).
- ³⁰ R. Sharma, S. D. Edkins, Z. Wang, A. Kostin, C. Sow, Y. Maeno, A. P. Mackenzie, J. C. S. Davis, and V. Madhavan, Momentum-resolved superconducting energy gaps of Sr_2RuO_4 from quasiparticle interference imaging, *Proc. Natl. Acad. Sci. USA* **117**, 5222 (2020).
- ³¹ G. Eilenberger, Transformation of Gorkov's equation for type II superconductors into transport-like equations, *Z. Physik* **214**, 195–213 (1968).
- ³² N. Schopohl and K. Maki, Quasiparticle spectrum around a vortex line in a d -wave superconductor, *Phys. Rev. B* **52**, 490 (1995).
- ³³ M. Eschrig, Distribution functions in nonequilibrium theory of superconductivity and Andreev spectroscopy in unconventional superconductors, *Phys. Rev. B* **61**, 9061–9076 (2000).
- ³⁴ M. Eschrig, Scattering problem in nonequilibrium quasi-classical theory of metals and superconductors: General boundary conditions and applications, *Phys. Rev. B* **80**, 134511 (2009).
- ³⁵ Y. Tanaka, Y. Tanuma, and A. A. Golubov, Odd-frequency pairing in normal-metal/superconductor junctions *Phys. Rev. B* **76**, 054522 (2007).
- ³⁶ J. Hara and K. Nagai, A Polar State in a Slab as a Soluble Model of p -Wave Fermi Superfluid in Finite Geometry *Prog. Theor. Phys.* **76**, 1237 (1986).
- ³⁷ M. Diez, J. P. Dahlhaus, M. Wimmer, and C. W. J. Beenakker, *Phys. Rev. B* **86**, 094501 (2012).
- ³⁸ S.-I. Suzuki and Y. Asano, Effects of surface roughness on the paramagnetic response of small unconventional superconductors, *Phys. Rev. B* **91**, 214510 (2015).
- ³⁹ S. Ikegaya, S.-I. Suzuki, Y. Tanaka, and Y. Asano, Quantization of conductance minimum and index theorem, *Phys. Rev. B* **94**, 054512 (2016).
- ⁴⁰ Y.-S. Li, N. Kikugawa, D. A. Sokolov, F. Jerzembeck, A. S. Gibbs, Y. Maeno, C. W. Hicks, J. Schmalian, M. Nicklas, A. P. Mackenzie, High-sensitivity heat-capacity measurements on Sr_2RuO_4 under uniaxial pressure, *Proc. Natl. Acad. Sci. USA* **118**, e2020492118 (2021).
- ⁴¹ S. Kashiwaya, K. Saitoh, H. Kashiwaya, M. Koyanagi, M. Sato, K. Yada, Y. Tanaka, and Y. Maeno, Time-reversal invariant superconductivity of Sr_2RuO_4 revealed by Josephson effects, *Phys. Rev. B* **100**, 094530 (2019).